

Plasma-grains interaction mediated by streaming non-Maxwellian ions

Sita Sundar¹ and Zhandos A. Moldabekov^{2,3}

¹*Department of Aerospace Engineering, Indian Institute of Technology Madras, Chennai - 600036, India*

²*Institute for Experimental and Theoretical Physics,*

Al-Farabi Kazakh National University, 71 Al-Farabi str., 050040 Almaty, Kazakhstan and

³*Institute of Applied Sciences and IT, 40-48 Shashkin Str., 050038 Almaty, Kazakhstan*

A comprehensive parametric study of plasma-grain interaction for non-Maxwellian streaming ions in steady-state employing particle-in-cell simulation is delineated. Instead of considering the inter-grain interaction potential to be the linear sum of isolated grain potentials, we incorporate the numerical advancement developed fully for grain shielding by including nonlinear contributions from plasma and shadowing effect. The forces acting on grains versus inter-grain distance and streaming velocity of ions as well as impact of trapped ions density (number) is characterized for non-Maxwellian ions in the presence of charge-exchange collisions. It is found that the nonlinear plasma response considerably modifies the plasma-grains interaction. Unlike the stationary plasma case, for two identical grains separated by a distance, electrostatic force is neither repulsive for all grain separations nor equivalent to the force due to one isolated grain. Inadequacy of the linear response formalism in dealing with the systems having higher grain charges is also discussed. The smallest inter-grain separation for which the role of the shadow effect can be ignored is reported.

I. INTRODUCTION

Dusty (complex) plasma is characterized by the presence of highly-charged dust particulates with sizes ranging from tens of nanometers to hundreds of microns in addition to ions, neutrals, and highly mobile electrons. These charged particulates impart features to the complex plasma physics leading to self-organization of dust particles, propagation and instabilities of low-frequency dust particle waves [1–6], formation of voids in experiments under micro-gravity conditions [7], ion-focusing and formation of dust induced wakes [8–13].

Wakefield drastically modifies interaction between charged particles [9, 14, 15]. Dynamics of a grain in streaming plasma and wake formation is a problem of fundamental research interest and is one of the most discussed problems (e.g., see [16, 17]) due to importance for a variety of applications ranging from fusion-related research [18–20] to astrophysical topics [21], operation of gas discharges [22], understanding Langmuir probes [23], and technological plasma applications [24, 25]. Particularly, in radio-frequency (rf) discharge experiments, dust particulates develop near sheath region where ions have non-zero streaming speeds due to the prevailing large-scale electric field.

Impact of ion streaming on inter-grain interaction is illustrated here with a in Fig. 1. In subplot we have shown (a) two stationary grains isotropically screened by ions in stationary plasma. Subplot (b) exhibits two-grains of same radii in streaming plasmas. It can be observed that ions can be intercepted by the grain or by an excess ion density focused downstream that could have otherwise bombarded the second grain (notice the dashed arrow towards downstream grain). From the subplots of Fig. 1, one can observe that the difference in the two cases emphasize the crucial role played by streaming.

The grain-plasma system in close proximity to the grain constitutes an open system (as illustrated in Fig. 1) [26–

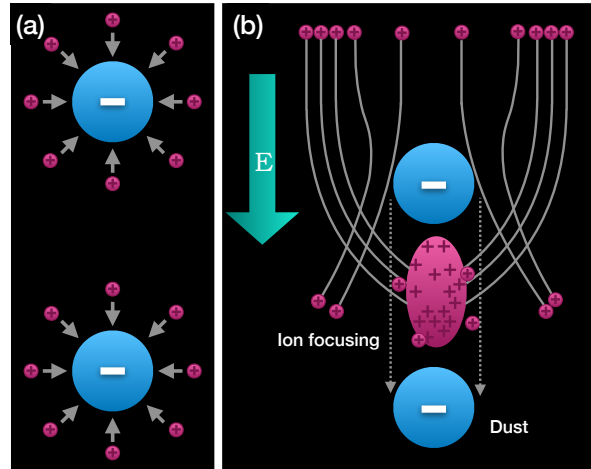


FIG. 1. Schematic illustrating (a) a system of two stationary grains surrounded with ions isotropically (b) an anisotropic system of two stationary grains in streaming ions in the presence of external driving field.

28], which forbids the calculation of interaction force directly from the derivative of electrostatic potential [29]. Important effect due to finite size of dust particles is a non-electrostatic force better named as ‘shadowing force’ which has mechanical origin [30, 31]. This shadowing force could be understood as the net ion-bombardment force exerted on a grain towards every other grain in its proximity due to the ions intercepted by each other. It is not a pairwise interaction force in the strict sense as it depends on the mutual alignment of the two or more grains and on their sizes. Work in this regard has been performed notably by Lampe *et al.* [29] wherein they introduced the role of nonlinearity and ‘shadowing force’ for simulating inter-grain interactions in stationary plasma and defied previous unjustified assumptions. For the case of grains in stationary plasma, Lampe *et al.* [29] showed

that the role of trapped ions in manifesting any kind of attractive inter-grain interaction is negligible and concluded that the electrostatic force between grains is always repulsive for the Maxwellian or shifted Maxwellian distribution of ions.

In the presence of an electric field driving the ion flow and ion-atom collisions (as is the case in the sheath region), the steady state ion velocity distribution is quite different from the Maxwellian and shifted Maxwellian distribution. The balance between electric field driven force and drag due to ion-neutral charge exchange collisions (the predominant collision) determine the flow velocity and the ion flow distribution function. It has been shown using Monte-Carlo (MC) numerical scheme [32] that the resulting distribution for ions is non-Maxwellian. Under constant ion-neutral charge-exchange collision frequency assumption, an exact solution for the distribution function reads [8, 9, 32],

$$f_z(u_z) = \frac{1}{2M_{\text{th}}} \exp\left(\frac{1 - 2M_{\text{th}}u_z}{2M_{\text{th}}^2}\right) \times \left[1 + \operatorname{erf}\left(\frac{M_{\text{th}}u_z - 1}{\sqrt{2}M_{\text{th}}}\right)\right], \quad (1)$$

here $u_z = v_z/v_{\text{th}}$ denotes the velocity along the streaming direction in the units of the thermal velocity of neutrals, v_{th} , and $M_{\text{th}} = v_d/v_{\text{th}}$ stands for the thermal Mach number with v_d being the drift velocity of ions.

For better understanding of the inter-grain interaction, the non-Maxwellian ion distribution and nonlinear plasma response to the field of grains have to be taken into account. Therefore, the purpose of the present work is to provide a consistent wide ranging numerical exploration of the forces acting on grains and plasma-grain interaction using the particle-in-cell numerical approach. For two dust particles aligned along streaming velocity (see Fig. 1), we simultaneously consider the impact of the following effects on grain-grain interactions :

- the non-Maxwellian velocity distribution of ions ;
- the trapped ions in the vicinity of the grain;
- the shadowing effect due to close location of grains;
- the non-linear response of the plasmas.

The outline of the paper is as follows. In Sec. II and III, we introduce plasma parameters and simulation scheme utilized, respectively. In Sec. IV, we present the results for dust particles charges and inter-grain interaction. Finally, in Sec. V. we discuss the perturbation of the density distribution of ions.

II. PLASMA PARAMETERS

The investigation has been done at the following plasma parameters:

1. Electron temperature $T_e = 3$ eV, ion and neutral (Ar) temperature $T_i = T_n = 0.03$ eV, $T_e/T_n = 100$, plasma density $n_e = n_i = 1 \times 10^8$ cm⁻³, neutrals density (pressure) $n_n = 5 \times 10^{14}$ cm⁻³ ($P = 2$ Pa), the Debye length due to electrons $\lambda_{De} = 1286.9$ μm , the Debye length due to ions $\lambda_D = 128.69$ μm , sound speed $c_s = \sqrt{T_e/m_i} = 2.68 \times 10^5$ cm, and the ion charge number $Z_i = 1$.
2. The molecular species is Ar and is considered to be kept at a collision frequency which is related to the collision cross-section through $\nu_{in} = \sigma_{in}n_n v_{th}$ where σ is the collision cross-section. The latter has been chosen to be equal to $\sigma_{in} = 3.5 \times 10^{-15}$, correspondingly the charge-exchange ion-atom collision frequency turns out to be $\nu_{in} = 4.69 \times 10^4$ s⁻¹. At considered plasma parameters, plasma frequency of ions $\omega_{pi} = 44.56 \nu_{in}$.
3. The dust particle has a cylindrical shape but with the diameter equal to the length. The dust particle radius $a_d = 5$ μm , separation between dust particles d/λ_D is varied from 2.02 to 10.1 with the step 2.02. Note that the grain radius is much smaller than the screening length, i.e., $\lambda_{De}/a_d = 257.382$ and $\lambda_D/a_d = 25.74$.
4. Ion streaming velocity considered herein encompasses the subsonic, sonic as well as supersonic regimes. The thermal Mach number $M_{\text{th}} = 0, 5, 10, 15$ is in the range from 0 to 15. The corresponding Mach number defined by the sound speed $M = M_{\text{th}} \sqrt{T_n/T_e}$ varies in the range from 0 to 1.5.

III. NUMERICAL DETAILS

We consider a homogeneous plasma with ion flow driven by uniform ambient electric field, E_0 (as indicated in Fig. 1). Balance of the electric field and ion-neutral charge-exchange collisions, ν_{in} , determine the ambient velocity distribution of ions, Eq. (1). The driving electric field is related to the charge-exchange collision frequency through the relation $qE_{\text{drift}} = m_i \nu_{in} v_d$, where v_d is the drift speed of the ions, m_i and $q = Z_i e$ denotes the mass and charge of the ion, respectively.

Numerical simulation has been performed with the two-dimensional (r,z) cylindrical Particle-In-Cell (PIC) code ‘DUSTrz’ [29], where the grains are kept stationary. In ‘DUSTrz’, the grain-grain separation and size could be varied and the dynamics of plasma is studied by following the motion of ions. Ions are PIC super-particles and electrons are taken to be thermal, i.e., the electron density is given by Boltzmann distribution $\tilde{n}_e = n_e \exp(e\phi/T_e)$. We have followed cgs unit for all physical parameters except temperatures which are in eV.

The equation to delineate the dynamics of the ions in the presence of self-consistent electric fields and driving electric field is given by

$$m_i \frac{d\mathbf{v}}{dt} = q [\mathbf{E}_{\text{pl}} + \mathbf{E}_{\text{grain}}], \quad (2)$$

here \mathbf{E}_{pl} is the field due to plasma (both electrons and ions), $\mathbf{E}_{\text{grain}}$ is the field due to dust grains. The ions crossing the boundary of the simulation box are replaced by an ion chosen randomly in accordance with the ambient distribution. This way, the code is capable of incorporating a chosen distribution. We use non-Maxwellian distribution given by Eq.(1). Note that to avoid double counting the driving field $\mathbf{E}_{\text{drift}}$ is not included explicitly in Eq. (2).

Simulation region is deliberately chosen to be very large ($50\lambda_D$ along radial direction and $200\lambda_D$ along the z -direction) to mitigate boundary effects. At the boundaries, electrostatic potential is set to zero. Plasma space charge density along with grain charge density constitutes the source term for Poisson's equation. Poisson's equation was solved in the given cylindrical simulation region at every ten time-steps. To facilitate the calculation of Poisson's equation, grains are considered to have uniform charge density at all points on the grain surface and any variation in the potential on the grain surface has been ignored. Moreover, one needs to resolve the ion dynamics in the vicinity of the grain and hence, the time-step has been chosen to be small $dt < (a_d/c_s)$ accordingly.

For computation of the dust particle charge, forces acting on dust particles for the non-Maxwellian ion distribution, the system is evolved self-consistently for 3000000 time-steps and averaging is done over every 40000 time-steps. The weight used for simulation particles is of the order of unity and hence it is suitable for obtaining sufficient statistics of the particle motion.

The present model is advanced in the sense that it doesn't consider the total potential for a system of two dust grains in streaming ions as linear sum of the potential due to two Debye spheres rather simultaneously takes into account the effect of trapped ions, shadowing force, and nonlinear response of plasmas as well.

Electrical force acting on each dust particle have been calculated as $Q_{1(2)} (\mathbf{E}_{2(1)}(z_{1(2)}) + \mathbf{E}_{\text{pl}}(z_{1(2)}))$, where $\mathbf{E}_{1(2)}$ is the field due to grain 1 (2), \mathbf{E}_{pl} is the field due to plasma. The dust particles are located along z axis (which is parallel to the drift velocity, see Fig. 1), where $z_1 = 0$ and $z_2 = d$ (with d being dust particles separation distance). In addition to the force due to grain charge and plasma, there is an additional force incorporated in the code in the same electrostatic force. This additional force which is also called ion drag, is due to the momentum deposition on the grains by ions traversing in the close proximity through Coulombic interactions. Moreover, electrostatic force here also takes care of the ions which get accelerated while passing in the neighborhood of the grain and fall into the electrostatic potential of the grain.

Plasma absorption induced force is the net rate of z -momenta deposited on the grain and is computed by depositing the momenta on to a grain whenever an ion collides with a grain. It includes the momentum transfer due to the ions whose trajectory got intercepted by

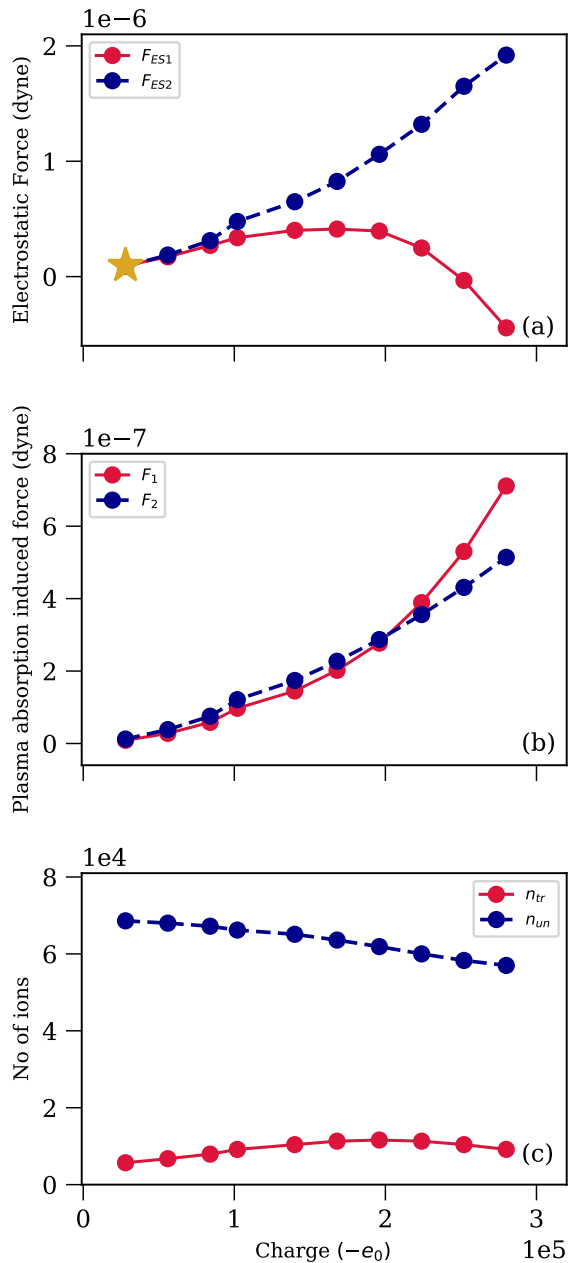


FIG. 2. Inter-grain (a) Electrostatic forces, (b) Plasma absorption induced forces, and (c) number of trapped and untrapped ions as a function of charges assigned to the grains for $M_{th} = 10$. The charge on unit of electron is denoted by e_0 here. The inter-grain distance is fixed to $d/\lambda_D = 6.06$.

the other grain as well as the ions passing nearby grain whose trajectory is focused on the other grain surface. Due to symmetry, we calculate the momentum deposition along flow direction only. In the equilibrium plasma ($M = 0$), the plasma absorption induced force is referred to as the shadow force, as one dust particle shadows the plasma flux on the surface of the second dust particle. In the case of single dust particle or very large separation

between dust particles, shadow force disappears. However, for the case of streaming plasmas ($M \neq 0$), there is ion drag force which has one component due to scattered ions and the second component due to absorption of ions. Former is included into the mentioned electrostatic force and latter contributes to what we call here the plasma absorption induced force. For two dust particles located close enough in streaming plasmas, the shadow force and plasma absorption related ion drag force can not be separated numerically from each other the way it is done theoretically.

We also computed the trapped and untrapped ions density (number). An ion is considered trapped ion if its total energy is negative. Number of untrapped ions is counted by integrating the difference between the average ion density and untrapped (with positive total charge) ions density.

IV. DUST PARTICLE CHARGES AND FORCES

Considering different values of the dust particle charge allows to illuminate the manifestation of the shadowing effect and non-linear plasma response. We have assigned linearly increasing charges on the grain and have measured the inter-grain forces and number of the trapped and untrapped ions. The plot of inter-grain force versus the charge assigned is plotted in Fig. 2, where the inter-grain distance is fixed $d/\lambda_D = 6.06$. From the subplot (a) of Fig. 2, we clearly see that with the increase of the dust particle charge from 10^4 (denoted by a star) to 10^5 the forces (directed downstream) acting on the dust particles increase approximately linearly. Further increase in the dust particles charge clearly shows strong non-linear dependence of the force on the dust particle charge at $Z_d > 10^5$. In this strong non-linear regime, the electrostatic force acting on the downstream particle (denoted as F_{ES2}) continues to increase while the upstream particle (denoted as F_{ES1}) exhibits a non-monotonic behavior. It first increases with grain charge till it reaches its maxima where it saturates followed by a decreasing trend eventually changing its sign upon further increase in the grain charge. The latter behavior is due to the formation of a negative charge region behind the grain (in downstream direction) as a result of the strong absorption of ions on the surface of the dust particles [33]. In a number of works, this effect was reported previously for a single dust particle in the flowing plasmas (e.g., [33, 34]). Here, we show this effect for two dust particles in plasmas with non-Maxwellian distribution of ions. Interestingly, the electrostatic force acting on downstream particle does not change its sign.

In the subplot (b) of Fig. 2, the plasma absorption induced force is presented. With the increase in the dust particle charge, the plasma absorption induced force increases for considered values of the dust particle charge. Except the region around point at which the electrostatic force acting on the upstream particle changes its sign,

the absorption induced force is approximately smaller by one order of magnitude. In the subplot (c) of Fig. 2, the number of trapped and untrapped ions is shown. The number of trapped ions exhibit a very small variation and number of untrapped ions decreases insignificantly with increase in the dust particle charge. This may seem somewhat counter-intuitive at first glance, but easily can be understood by recalling that the excess plasma (ions and electrons) density around dust particles is strictly controlled by the plasma quasi-neutrality condition [35], better understanding can be gained by looking at the pattern of the plasma distribution around dust particles. The latter is discussed in Sec. VI.

The described dependence of the forces on the dust particle charge clearly illustrates its significance for the variety of the possible phenomena. Further, we consider the forces acting on the dust particles by computing the dust particle charge self-consistently.

In the presence of streaming ions, two grains with the same size can collect different charges depending on the inter-grain separation. We also notice the non-reciprocal behavior of forces for the two grains. Unlike the case of two identical stationary grains in stationary ions [29], for the streaming ions the force on one grain exerted due to the other is no longer the same as the force exerted due to the field of an isolated grain exerting on the bare charge of the other. Flow velocity of ions, inter-grain separation, and non-linearity of plasma in the vicinity of the grain has a crucial role in determining the steady state charge of the grains.

To understand the inter-grain and plasma-grain interactions, in Fig. 3 we have shown the grain charges and the forces acting on grains for various values of the streaming velocity and inter-grain separation. The leftmost column shows the grain charge (in units of electron charge) versus inter-grain separation distance (in units of λ_D) for ions with $M_{th} = 0, 5, 10, 15$ (from top to bottom) respectively. For $M_{th} = 0$ (subplot(a)), the grain charges on both the grains are almost equal in the steady-state for all the inter-grain separation distances. In the remaining three subplots in the left column, the charge on the upstream particle (grain 1) is always higher in magnitude than the downstream particle (grain 2) implying that the downstream particle charges less negatively for $M_{th} \neq 0$. This is due to the fact that with streaming ions, focusing of ions occur downstream giving rise to smaller negative charge for the downstream grain. Though the charge on the grain 1 is more than grain 2 for all separations for streaming ions ($M_{th} \neq 0$), nevertheless the difference between the two grain charges asymptotes to zero at very large separations where one expects the shadowing and focusing effects to be negligible. At smaller separations, the difference between grain charges increases with streaming ion speeds. In general, the pattern exhibited by grain-charge with respect to inter-grain separation distance is due to the synergistic role played by shadow force and plasma streaming.

Electrostatic force versus grain separation is shown in the

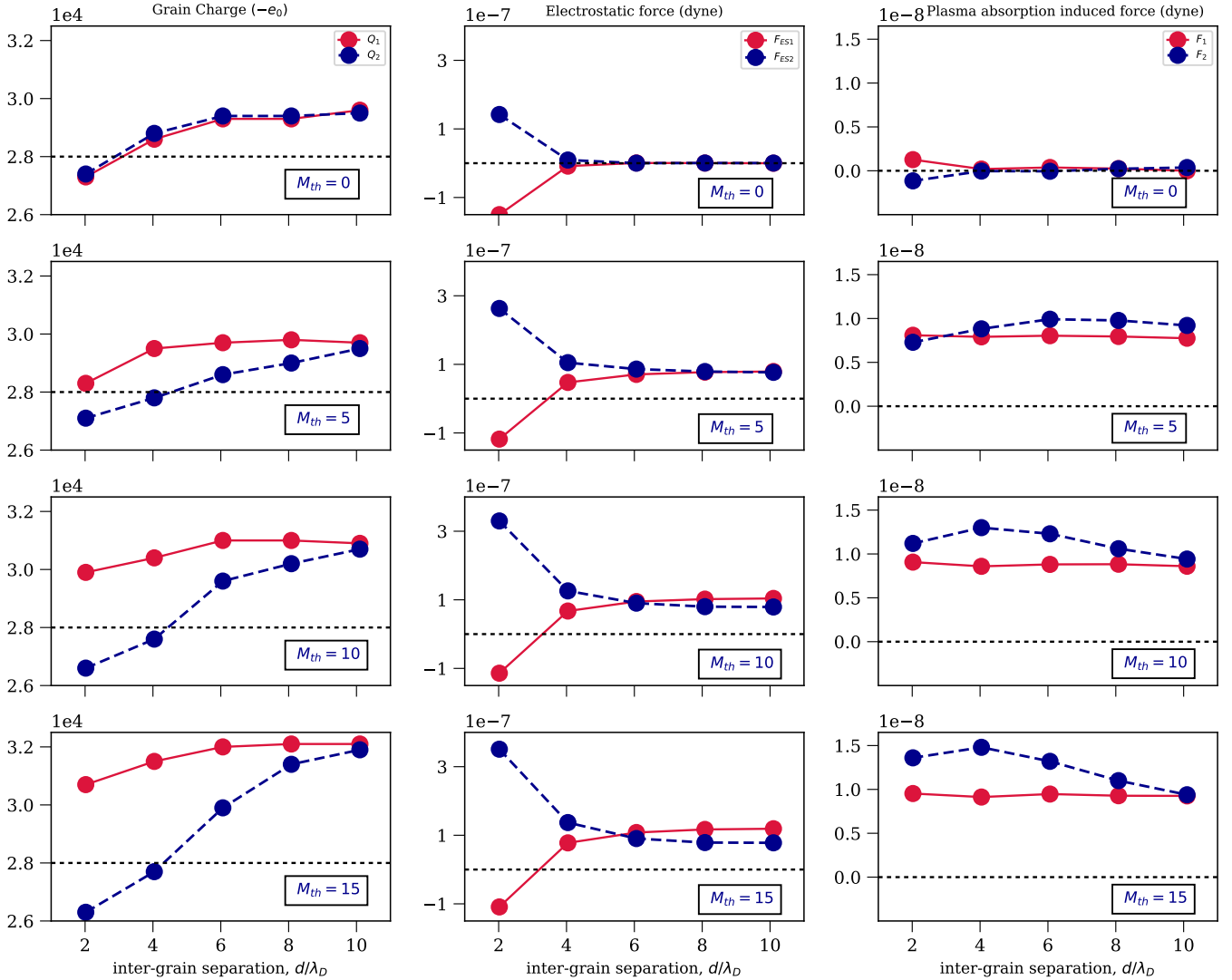


FIG. 3. Grain charge (left column), Electrostatic force (middle column), and Plasma induced absorption force (right column) as a function of separation distance between the particles for $M_{th} = 0$, $M_{th} = 5$, $M_{th} = 10$, and $M_{th} = 15$. The black dashed horizontal line shown in the four subplots (left column) display the initial grain charge of $28000e_0$ where e_0 is the charge on one electron. The black dashed lines in the middle and right column indicates line at the value zero.

second (middle) column of Fig. 3. In the case $M_{th} = 0$, the force acting on the upstream grain is opposite to the force acting on downstream grain. Similarly, at $M_{th} \neq 0$ and $d/\lambda_D = 2.02$, the electrostatic force on grain 1 is asymmetrically opposite to grain 2. In these cases the Coulombic repulsion between dust particles is stronger than the ion drag force. The total force acting on the system of two dust particles is zero in the case $M_{th} = 0$ and non-zero in the case $M_{th} \neq 0$. As it is expected, electrostatic force is significant at smaller inter-grain separations and is weaker at larger separations. At $M_{th} = 10$ and $M_{th} = 15$, at distances $d/\lambda_D \geq 6$, the electrostatic force acting on upstream particle (grain 1) becomes greater than that acting on downstream particle (grain 2). This means that at smaller grain separations (usually

$d \leq 6.06\lambda_D$) the electrostatic force exerts a pull on the downstream particle to bring it closer to the upstream particle while at larger grain separations $d \geq 6.06\lambda_D$ electrostatic force is trying to push upstream particle closer to the downstream particle.

Additionally, the magnitude of electrostatic force is higher than plasma absorption induced force (see right-most column) for all the grain separation distances. So, we can say that the electrostatic force is the dominant force as its magnitude is always larger than the shadow force. Note that the opposite situation may accrue at significantly larger grain charges (sizes) as it is illustrated in Fig. 2.

The plasma absorption induced force versus grain separation is shown in Fig. 3 (last column). For $M_{th} = 0$,

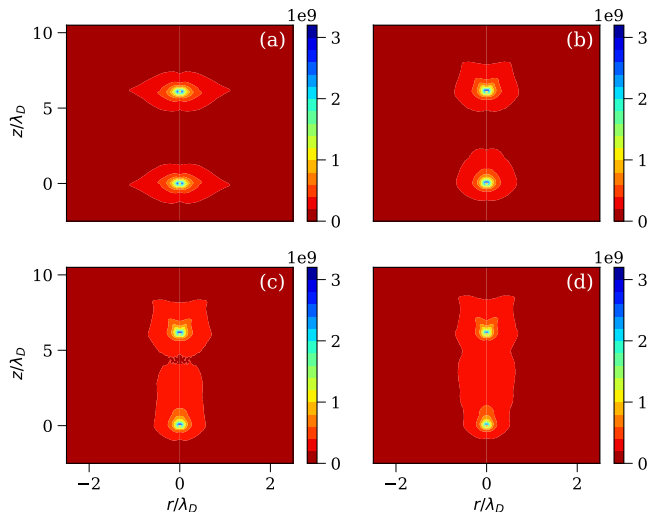


FIG. 4. Spatial profiles of the ion density for (a) $M_{th} = 0$, (b) $M_{th} = 5$, (c) $M_{th} = 10$, and (d) $M_{th} = 15$, for a non-Maxwellian drift distribution with inter-grain separation $d/\lambda_D = 6.06$. The plasma conditions are same as in Fig 3.

the plasma absorption induced force is referred to as the shadow force. In this case the shadow force acting on grain 1 is asymmetrically opposite to grain 2, meaning that shadow force tends to attract dust particles to each other. At very small separation, $d = 2.02\lambda_D$, it has positive value for downstream grain and equal negative value for upstream grain.

For non-Maxwellian distribution with streaming ions, at relatively small distance between grains, the ion drag component due to plasma absorption on the surface of the dust particles can not be separated from the shadow force. However, at large enough distances between grains, the shadowing effect vanishes as the problem reduces to the two isolated from each other grains. Indeed, at $d/\lambda = 10.1$, for the considered case of equal sized dust particles, the plasma absorption induced force is almost same for both upstream and downstream particles. In this case the plasma absorption induced force is the ion drag force component due to absorption of ions on the surface of the grain. At $M_{th} \neq 0$, the plasma absorption induced force is always positive (meaning directed along streaming), implying that the ion drag force component due to absorption is always dominant over shadow force.

V. IONS PERTURBATION BY DUST PARTICLES

Fig. 4 shows the 2D ion density distribution around dust particles for (a) $M_{th} = 0$, (b) $M_{th} = 5$, (c) $M_{th} = 10$, and (d) $M_{th} = 15$ at the inter-grain separation $d/\lambda_D = 6.06$. For (a) $M_{th} = 0$, one can see well separated plasma polarization (symmetric in both r and z) around the two grains. However, as one increases the ion stream-

ing speed, the shielding around the two grains overlap each other and finally becomes anisotropic (asymmetric in z) (subplot (d)). With increase in streaming ion speed, the size of the polarized ion cloud around dust particles increases as ions become scattered to large distances (smaller angles).

Indeed, this can be seen from Fig. 5, where ion density (trapped as well as untrapped) versus grain separation is shown. Trapped ions are the ions collected by the grain which have a total negative energy. Subplots (a) and (b) show the trapped and untrapped density respectively for the above mentioned four cases (similar to Fig. 3). The upstream dust particle (grain 1) is located at $z = 0$ and the second dust particle (grain 2) is positioned at $z = d$. From Fig. 5, one can see that the downstream excess ion density has monotonically decaying character without clearly distinct (separated) focused ion cloud. For a single dust particle, with non-Maxwellian ion distribution, such pattern was previously reported in Ref. [35] on the basis of the linear response approach. Here, we confirm this pattern for the case of two dust particles beyond linear approximation. Overall, the trapped ion density does not show strong variation with change in the streaming velocity from $M_{th} = 5$ to $M_{th} = 15$. Nevertheless, one can note here the localized nature of trapped ions around grains and spreading of untrapped ions with streaming ion velocity downstream grain. The untrapped ion density for streaming ions shows a sharp front and a long ion density tail. Two peaks (in red color one at $z = 0$ and other at $z = 2.02\lambda_D$) shows the density around two grains. The peak of the first grain for all grain distances overlap at $z = 0$.

Additionally, it can be seen from Fig. 5, the trapped ion density does not show much variation with change in inter-grain separation. This is in agreement with the computed value of grains charge, which also does not change drastically with increase in Mach number and the separation distance between grains. Note that the trapped ions, having high probability to fall on the surface of dust particle, is correlated with the charge of the dust particles.

For $M_{th} = 5$, similar to the trapped ions case, the untrapped ion density does not exhibit a significant variation with increase in inter-grain separation. However, at higher values of streaming velocity, $M_{th} = 10$ and $M_{th} = 15$, the untrapped ion density has its maximal values at $d/\lambda_D = 4.04$ (see Fig. 5). One point which is noteworthy is that both trapped and untrapped ion density peaks around $d = 6.06\lambda_D$ for subsonic flows. This peak shifts towards $d = 4.04\lambda_D$ as we increase the flow strength. This is in coherence with our observation of electrostatic and ion absorption induced force behavior which exhibit attractive behavior around $d = 6.06\lambda_D$ for $M_{th} = 5$ and the critical distance shifts towards smaller inter-grain separation as one increases the streaming speed of ions.

In Fig. 6, the number of trapped and untrapped ions is shown for different values of Mach number and inter-

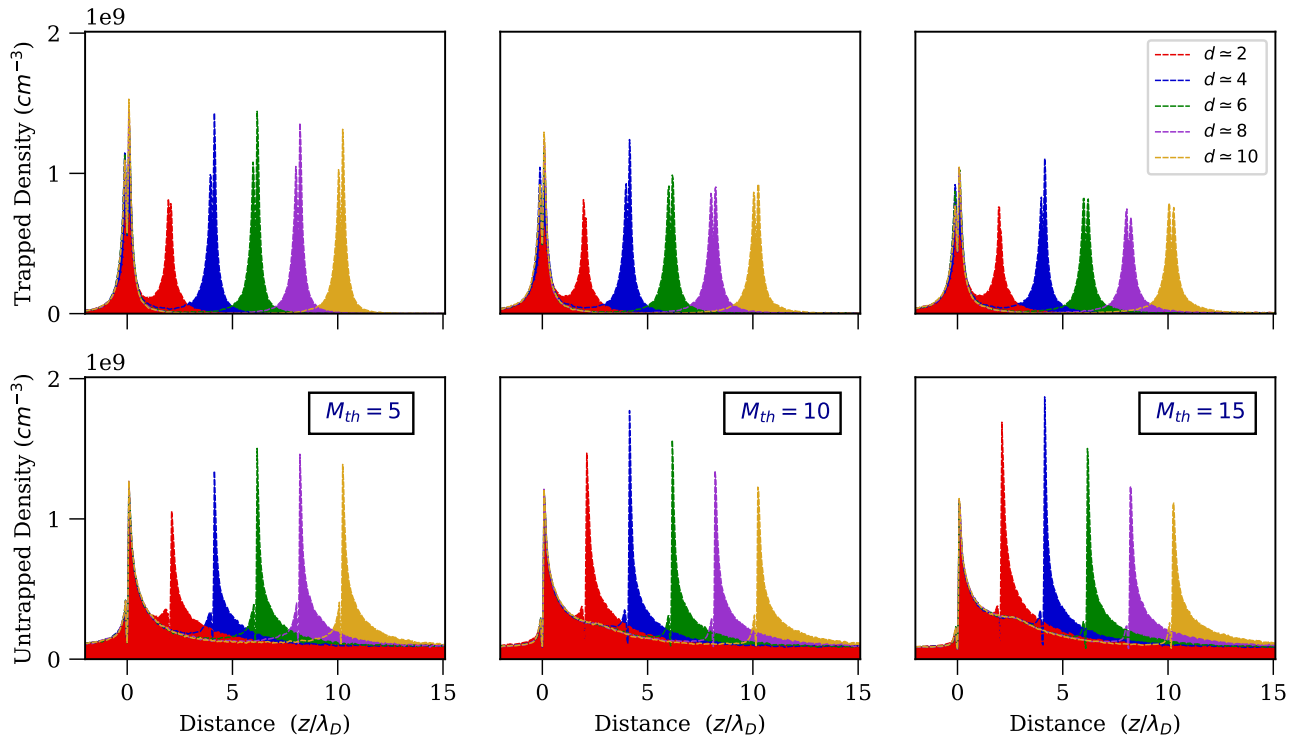


FIG. 5. Variation of the (a) trapped and (b) untrapped ion density along the flow direction for the the two grains. First (upstream) grain is at origin and the second (downstream) grain is placed at different locations $d/\lambda_D \sim 2, 4, 6, 8, 10$ for $M_{th} = 5$ (left column), $M_{th} = 10$ (middle column), and $M_{th} = 15$ (right column).

grain separation distance. The number of untrapped ions is computed by considering the difference in the average ion density and the untrapped ion density. Both trapped and untrapped number of ions is approximately constant for all values of the inter-grain separation distance. With increase in the Mach number from 0 to 10, the number of trapped ions increases. Further increase to $M_{th} = 15$ leads to slightly smaller number of trapped ions in comparison with the case $M_{th} = 10$. Note that the ions passing in the vicinity of the dust particles can lose their energy due to charge-exchange collision. Therefore, described non-monotonic dependence of the trapped ions number on Mach number can be understood as the competition between the effects of stronger influx of ions and higher escaping ability with increase in the Mach number.

The number of the untrapped initially increases with increase in ion streaming speed from 0 to 5 while it exhibits decreases with increase in the Mach number from 5 to 15 following as can be seen from the bottom panel of Fig. 6. Here, the increase of the untrapped ion number with increase of the Mach number from 0 to 5 can be explained by the effective ion focusing mechanism which dominates over the increase in the escaping ability of ions with increase in the Mach number. The latter mechanism becomes dominant with further increase in the Mach number from 5 to 15, leading to the decrease in the number

of the untrapped ions.

VI. CONCLUSIONS

We have presented here the study of grain charge and forces acting on grains at various parameters for non-Maxwellian ion flow distribution under typical experimental situations using particle-in-cell simulation scheme. As a result we observed that:

- The force-charge dependence does not show linear character for $Z_d \geq 10^5$.
- With increase in the streaming speed, the difference between the charge on the two grains increases while with increase in the inter-dust particle distance the difference between the charge on the two grains decreases.
- The plasma absorption induced force is not affected by the shadowing effect at $d/\lambda_D \geq 10$ and $M_{th} \leq 15$. At smaller inter dust distances, the shadowing effects can not be neglected if the plasma absorption induced force is considered.
- The shadowing effect has weak impact on the electrostatic force acting on two dust particles at $d/\lambda_D \geq 6$ and $M_{th} \leq 15$.
- The number of both trapped and untrapped ions remain approximately constant with increase in the

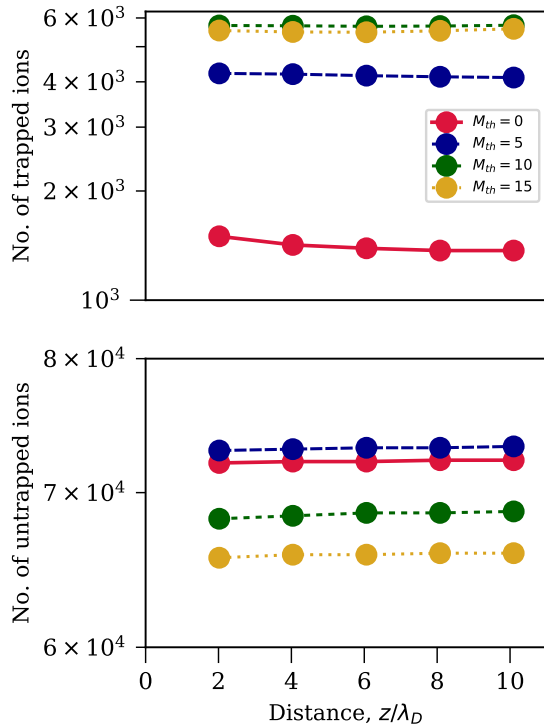


FIG. 6. Plot exhibiting number of (a) trapped and (b) untrapped ions as a function of separation distance between the particles for $M_{th} = 0$ (red circle - solid line), $M_{th} = 5$ (blue circle - big dashed line), $M_{th} = 10.0$ (green circle - small dashed line), and $M = 15$ (yellow circle - dotted line). The plasma conditions are same as in Fig. 3.

inter-dust particle distance from $d/\lambda_D = 2.02$ to $d/\lambda_D = 10.1$.

- The ion density perturbation due to two dust particles has a monotonically decreasing tail in downstream direction.
- Unlike the case of identical stationary grain-pair in stationary Maxwellian ions [29], the electrostatic force for the identical grain-pair in streaming ions is no longer repulsive for grain separations $d/\lambda_D \geq 2.02$. It give an indication of the attractive force for the grain-pair and the possibility for the existence of a bound pair of grains as envisaged in the previous experiments [36].
- Trapped and untrapped ion density exhibits a peak

VII. ACKNOWLEDGEMENTS

SS would like to thank Dr. M. Lampe for support in using the code ‘DUSTrz’, and acknowledges the support and hospitality of CAU Kiel Germany and IIT Madras India. This work was supported by the DFG via SFB-TR24, Project A9 and DRDO project via project no. ASE1718144DRDOASAM. Zh. Moldabekov thanks the funding from the Ministry of Education and Science of the Republic of Kazakhstan via the grant BR05236730 “Investigation of fundamental problems of Phys. Plasmas and plasma-like media” (2019).

-
- [1] O. Ishihara and S. V. Vladimirov, *Physics of Plasmas* (1994-present) **4**, 69 (1997).
- [2] A. Barkan, R. L. Merlino, and N. D’angelo, *Physics of Plasmas* **2**, 3563 (1995).
- [3] P. K. Kaw and A. Sen, *Physics of Plasmas* **5**, 3552 (1998).
- [4] T. S. Ramazanov, Z. A. Moldabekov, and M. T. Gabdullin, *Phys. Rev. E* **93**, 053204 (2016).
- [5] P. Bandyopadhyay, G. Prasad, A. Sen, and P. K. Kaw, *Phys. Rev. Lett.* **101**, 065006 (2008).
- [6] S. Kumar and A. Das, *Phys. Rev. E* **97**, 063202 (2018).
- [7] M. Kretschmer, S. A. Khrapak, S. K. Zhdanov, H. M. Thomas, G. E. Morfill, V. E. Fortov, A. M. Lipaev, V. I. Molotkov, A. I. Ivanov, and M. V. Turin, *Phys. Rev. E* **71**, 056401 (2005).
- [8] S. Sundar, H. Kaehlert, J.-P. Joost, P. Ludwig, and M. Bonitz, *Physics of Plasmas* (2017).
- [9] P. Ludwig, H. Jung, H. Kaehlert, J.-P. Joost, F. Greiner, Z. Moldabekov, J. Carstensen, S. Sundar, M. Bonitz, and A. Piel, *The European Physical Journal D* **72**, 82 (2018).
- [10] S. Sundar, *Phys. Rev. E* **98**, 023206 (2018).
- [11] S. Sundar, *Physical Sciences and Technology* **5**, 16 (2018).
- [12] G. E. Morfill and A. V. Ivlev, *Rev. Mod. Phys.* **81**, 1353 (2009).
- [13] S. K. Kodanova, T. S. Ramazanov, N. K. Bastykova, and Z. A. Moldabekov, *Physics of Plasmas* **22**, 063703 (2015).
- [14] Z. A. Moldabekov, P. Ludwig, J.-P. Joost, M. Bonitz, and T. S. Ramazanov, *Contributions to Plasma Physics* **55**, 186 (2015).
- [15] Z. A. Moldabekov, P. Ludwig, M. Bonitz, and T. S. Ramazanov, *Contributions to Plasma Physics* **56**, 442 (2016).
- [16] M. Lampe, G. Joyce, G. Ganguli, and V. Gavrichchaka, *Physics of Plasmas* **7**, 3851 (2000).
- [17] P. Ludwig, W. J. Miloch, H. Kaehlert, and M. Bonitz, *New Journal of Physics* **14**, 053016 (2012).
- [18] J. Winter, *Plasma Physics and Controlled Fusion* **46**, B583 (2004).
- [19] J. Sharpe, D. Petti, and H.-W. Bartels, *Fusion Engineering and Design* **6364**, 153 (2002).
- [20] S. Ratynskaia, C. Castaldo, E. Giovannozzi, D. Rudakov, G. Morfill, M. Horanyi, J. H. Yu, and G. Maddaluno, *Plasma Physics and Controlled Fusion* **50**, 124046 (2008).
- [21] J. S. Halekas, V. Angelopoulos, D. G. Sibeck, K. K. Khurana, C. T. Russell, G. T. Delory, W. M. Farrell, J. P. McFadden, J. W. Bonnell, D. Larson, R. E. Ergun, F. Plaschke, and K. H. Glassmeier, *Space Science Reviews* **165**, 93 (2011).

- [22] V. E. Fortov, A. P. Nefedov, V. I. Molotkov, M. Y. Poustylnik, and V. M. Torchinsky, *Phys. Rev. Lett.* **87**, 205002 (2001).
- [23] I. Hutchinson, *Physics of Plasmas* **15**, 123503 (2008).
- [24] P. Hartmann, Z. Donkó, G. J. Kalman, S. Kyrkos, K. I. Golden, and M. Rosenberg, *Phys. Rev. Lett.* **103**, 245002 (2009).
- [25] P. Hartmann, A. Douglass, J. C. Reyes, L. S. Matthews, T. W. Hyde, A. Kovács, and Z. Donkó, *Phys. Rev. Lett.* **105**, 115004 (2010).
- [26] V. A. Schweigert, I. V. Schweigert, A. Melzer, A. Homann, and A. Piel, *Phys. Rev. E* **54**, 4155 (1996).
- [27] A. Melzer, V. A. Schweigert, I. V. Schweigert, A. Homann, S. Peters, and A. Piel, *Phys. Rev. E* **54**, R46 (1996).
- [28] V. A. Schweigert, V. M. Bedanov, I. V. Schweigert, A. Melzer, A. Homann, and A. Piel, *Journal of Experimental and Theoretical Physics* **88**, 482 (1999).
- [29] M. Lampe and G. Joyce, *Physics of Plasmas* **22**, 023704 (2015).
- [30] V. N. Tsytovich, Y. K. Khodataev, and R. Bingham, *Plasma Physics and Controlled Fusion* **17** (1996).
- [31] A. M. Ignatov, *Plasma Phys. Rep.* **22**, 648 (1996).
- [32] M. Lampe, T. B. Röcker, G. Joyce, S. K. Zhdanov, A. V. Iylev, and G. E. Morfill, *Physics of Plasmas* **19**, 113703 (2012).
- [33] A. I. Momot, *Physics of Plasmas* **24**, 103704 (2017).
- [34] L. Patacchini and I. H. Hutchinson, *Phys. Rev. Lett.* **101**, 025001 (2008).
- [35] Z. A. Moldabekov, P. Ludwig, , and M. Bonitz, *Physical Sciences and Technology* **5**, 10 (2018).
- [36] A. Usachev, A. Zobnin, O. Petrov, V. Fortov, B. Annaratone, M. Thoma, H. Höfner, M. Kretschmer, M. Fink, and G. Morfill, *Physical review letters* **102**, 045001 (2009).